

Mater. Res. Soc. Symp. Proc. Vol. 1321 © 2011 Materials Research Society

DOI: 10.1557/opl.2011.1092

### High Efficiency, Large Area, Nanocrystalline Silicon Based, Triple-Junction Solar Cells

A. Banerjee, T. Su, D. Beglau, G. Pietka, F. Liu, B. Yan, J. Yang, and S. Guha  
United Solar Ovonic LLC, 1100 West Maple Road, Troy, MI, 48084, U.S.A.

#### ABSTRACT

We have fabricated large-area, thin-film multijunction solar cells based on hydrogenated amorphous silicon (a-Si:H) and nanocrystalline silicon (nc-Si:H) made in a large area batch reactor. The device structure consisted of an a-Si:H/nc-Si:H/nc-Si:H stack on Ag/ZnO back reflector coated stainless steel substrate, deposited using our proprietary High Frequency (HF) glow discharge technique. For the nc-Si:H films, we investigated two deposition rate regimes: (i) low rate  $<1$  nm/s and (ii) high rate  $>1$  nm/s. We optimized the deposition parameters, such as pressure, gas flow, dilution, and power. We did SIMS analysis on the optimized films, and found the impurity concentrations were one order of magnitude lower than the films made with the conventional RF process. In particular, the oxygen concentration is reduced to  $\sim 10^{18}$  cm<sup>-3</sup>. This value is among the lowest oxygen concentration reported in literature. The low impurity content is attributed to proprietary cathode hardware and the optimized deposition process. During the initial optimization and investigative phase, we fabricated small-area (0.25 cm<sup>2</sup> and 1.1 cm<sup>2</sup>) cells. The information obtained from the initial phase was used to fabricate large-area (aperture area 400 cm<sup>2</sup>) cells, and encapsulated the cells using the same flexible encapsulants that are used in our commercial product. We have light soaked the low-rate and high-rate encapsulated modules. The highest initial efficiency of the low-rate modules is 12.0% as confirmed by NREL. The highest corresponding stable efficiency attained for the low-rate samples cells is 11.35%. For the high-rate small-area (1.1 cm<sup>2</sup>) cells, the highest initial active-area efficiency and corresponding stable efficiency attained are 13.97% and 12.9%, respectively. We present the details of the research conducted to develop the low- and high-rate cells and modules.

#### INTRODUCTION

nc-Si:H material is a promising candidate to replace a-SiGe:H in multijunction thin film silicon solar cells [1-3]. In view of its indirect bandgap, the nc-Si:H layer must be much thicker than its amorphous counterparts to effectively absorb the incident radiation. Typical thicknesses for a nc-Si:H based multijunction cell is 2-5  $\mu$ m, compared with  $<0.5$   $\mu$ m for a corresponding a-Si:H/a-SiGe:H/a-SiGe:H triple-junction structure. While for commercial viability, the nc-Si:H layer must be deposited at a high rate, one must investigate the highest efficiency attainable with and without manufacturing constraint of deposition rate. In this paper, we report on this two-pronged strategy of fabricating large-area, high-efficiency a-Si:H/nc-Si:H/nc-Si:H solar cells at low and high rates.

To fabricate high-efficiency, large-area nc-Si:H based multijunction solar cells, it is necessary to first fabricate high quality nc-Si:H based component cells that exhibit excellent spatial uniformity of device thickness and device performance over a large area [4]. In particular, the bottom cell must meet stringent requirements in terms of short-circuit-current density ( $J_{sc}$ ), open-circuit voltage ( $V_{oc}$ ), and fill factor (FF). It has been suggested that oxygen

incorporated in the nc-Si:H absorbing layer is the major cause of loss in the long wavelength response: quantum efficiency (QE) at long wavelength and fill factor under red light [5,6]. We have developed a proprietary HF glow discharge technology to deposit the devices with good large area spatial uniformity and low impurity content. We have attained similar levels of oxygen concentration in nc-Si:H layers deposited at both low and high rates.

## EXPERIMENT

Large-area nc-Si:H single-junction and a-Si:H/nc-Si:H/nc-Si:H triple-junction solar cells were deposited using the HF process in a large-area batch reactor. The substrate consisted of a  $\sim 38$  cm x 35 cm piece of stainless steel coated with a back reflector of Ag/ZnO. For the nc-Si:H films, we investigated two deposition rate regimes: (i) low rate  $< 1$  nm/s and (ii) high rate  $> 1$  nm/s. We optimized the deposition parameters, such as pressure, gas flow, dilution, and power. During the initial optimization phase, the large-area coated substrate was cut into smaller pieces and ITO was deposited through an evaporation mask to delineate the device area. Two different device areas were used:  $0.25$  cm<sup>2</sup> and  $1.1$  cm<sup>2</sup>. For the  $0.25$  cm<sup>2</sup> devices, grid fingers were vacuum deposited for current collection. For the  $1.1$  cm<sup>2</sup> devices, grid wires and bus bars were applied for current collection. Device thickness, I-V characteristics, QE response, and their spatial uniformity were measured. Representative samples were sent out for impurity analysis and depth profiling using the SIMS technique. Finally, large-area (aperture area of  $400$  cm<sup>2</sup>) triple-junction cells were deposited. Grid wires and bus bars were applied for current collection. The large-area cells were encapsulated using our proprietary flexible encapsulants. The  $400$  cm<sup>2</sup> module is shown in Fig. 1.



**Figure 1.** A  $400$  cm<sup>2</sup> encapsulated module.

I-V characteristics of the large-area encapsulated modules were measured using a Spire solar simulator. The modules were light soaked under one-sun intensity at  $50$  °C and open-circuit conditions for 1000 hours. The modules in the initial and light stabilized states were sent to NREL for efficiency confirmation.

**DISCUSSION****Impurity levels in absorbing layers**

Reducing incorporation of impurities in the nc-Si:H absorbing layers is crucial to achieving high efficiency. It is well known that high levels of impurities, especially oxygen, in the absorbing layer can produce additional defect states that cause inferior long wavelength response. By continuing optimization of hardware, especially the HF cathode design, and deposition process, we have reduced the impurities in the absorbing layers to much lower levels. More importantly, we achieved very low impurity levels with both low and high deposition rates. Table I shows the impurity concentrations in the absorbing layer in the nc-Si:H bottom cells made at both low (<1 nm/s) and high (>1 nm/s) deposition rates.

**Table I.** Concentration of major impurities in the absorbing layer in nc-Si:H bottom cell made at low (<1 nm/s) and high (>1 nm/s) deposition rates. Shaded rows represent cells at low rate.

| Run #<br>3D | Impurity concentration (atom/cm <sup>3</sup> ) |                    |                    |                     |                    |
|-------------|--|--------------------|--------------------|---------------------|--------------------|
|             | oxygen   | carbon             | nitrogen           | boron               | fluorine           |
| 3D10451     | 2x10 <sup>18</sup>                             | 6x10 <sup>16</sup> | 5x10 <sup>15</sup> | <1x10 <sup>16</sup> | 2x10 <sup>15</sup> |
| 3D10455     | 1.2x10 <sup>18</sup>                           | 6x10 <sup>16</sup> | 5x10 <sup>15</sup> | <1x10 <sup>16</sup> | 2x10 <sup>15</sup> |
| 2B18283     | 1.5x10 <sup>18</sup>                           | 4x10 <sup>17</sup> | 1x10 <sup>17</sup> | <1x10 <sup>16</sup> | 2x10 <sup>15</sup> |
| 2B18687     | 1.5x10 <sup>18</sup>                           | 4x10 <sup>17</sup> | 1x10 <sup>17</sup> | <1x10 <sup>16</sup> | 2x10 <sup>15</sup> |

In Table I, the shaded rows represent cells made at low rate. The oxygen concentration is similar in cells deposited at both low and high rates. The low rate deposition produces very low concentrations of nitrogen and carbon. These are among the lowest impurity levels reported in nc-Si:H based cells.

**Low rate (<1 nm/s) cell: initial performance**

Table II lists the initial efficiencies of the large-area a-Si:H/nc-Si:H/nc-Si:H triple-junction modules with an aperture area of 400 cm<sup>2</sup> made at low deposition rate (<1 nm/s). These modules were measured at United Solar (USO) and at NREL under respective Spire solar simulators. The initial aperture-area efficiency ranges between 11.1-12.0% as measured by NREL. The agreement in efficiency between the two laboratories is within 4%. Modules 10554 and 10555 exhibit an efficiency of 12.0%. Figure 2 shows the NREL initial I-V characteristics of the two modules. This is the highest value as confirmed by NREL for a module of this size. The results also demonstrate the capability of the nc-Si:H technology to make high efficiency solar cells.

**Table II.** Initial efficiency of large-area (aperture area ~400 cm<sup>2</sup>) modules made at low deposition rate (<1 nm/s).

| Module #<br>3D | Measurement | Area<br>(cm <sup>2</sup> ) | Temp.<br>(°C) | V <sub>oc</sub><br>(V) | I <sub>sc</sub><br>(A) | FF<br>(%) | Efficiency<br>(%) |
|----------------|-------------|----------------------------|---------------|------------------------|------------------------|-----------|-------------------|
| 10527          | USO         | 400                        | 24.2          | 1.87                   | 3.43                   | 71.7      | 11.50             |
|                | NREL        | 399.8                      | 25.2          | 1.882                  | 3.525                  | 67.1      | 11.10             |
| 10529          | USO         | 400                        | 25.4          | 1.912                  | 3.36                   | 72.5      | 11.67             |
|                | NREL        | 399.8                      | 25.1          | 1.925                  | 3.5                    | 68.9      | 11.60             |
| 10554          | USO         | 400                        | 24.5          | 1.936                  | 3.41                   | 73.2      | 12.09             |
|                | NREL        | 399.8                      | 25.1          | 1.948                  | 3.57                   | 69.2      | 12.00             |
| 10555          | USO         | 400                        | 25.3          | 1.906                  | 3.53                   | 71.3      | 12.02             |
|                | NREL        | 399.8                      | 25.1          | 1.92                   | 3.676                  | 68.0      | 12.00             |

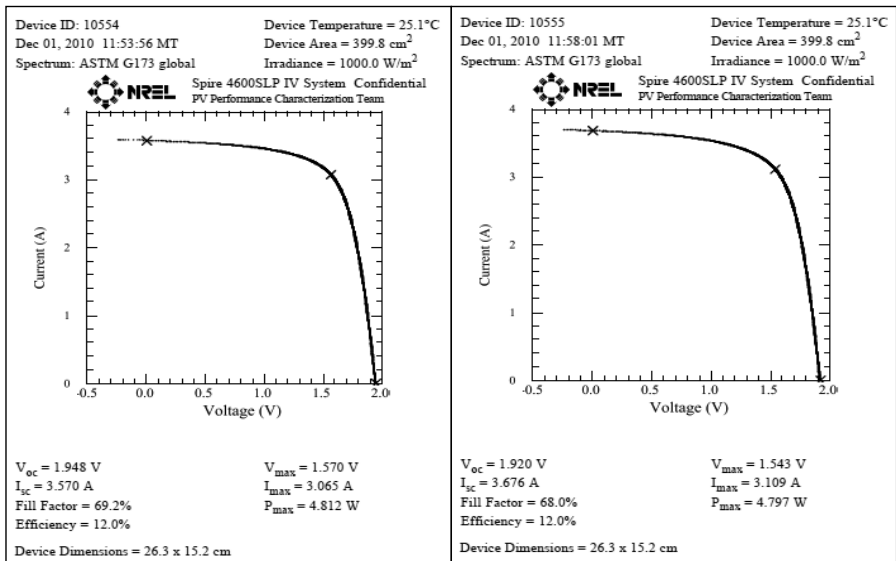


**Figure 2.** Initial J-V characteristics measured at NREL of the two highest efficiency (12.0%) a-Si:H/nc-Si:H/nc-Si:H encapsulated modules 10554 and 10555 shown in Table II.

**High rate (>1 nm/s) cell: initial performance**

We have fabricated small-area (1.1 cm<sup>2</sup>) a-Si:H/nc-Si:H/nc-Si:H triple-junction cells deposited at high rate (>1 nm/s). Table III shows the initial active-area J-V characteristics of the unencapsulated cells and the QE values for the component cells and the total device. The

efficiency (last column) is the active-area efficiency as calculated from the  $V_{oc}$ , FF, and limiting-current QE values in Table III. The efficiency is in the range of 13.67-13.97%.

**Table III.** Initial active-area efficiency of  $1.1 \text{ cm}^2$  unencapsulated cells deposited at  $>1 \text{ nm/s}$  as measured at USO.

| Cell ID   | $V_{oc}$ (V) | FF    | QE ( $\text{mA}/\text{cm}^2$ ) |        |        |       | Efficiency (%) |
|-----------|--------------|-------|--------------------------------|--------|--------|-------|----------------|
|           |              |       | Top                            | Middle | Bottom | Total |                |
| 18730D3-5 | 1.99         | 0.762 | 9.42                           | 9.7    | 9.13   | 28.3  | 13.81          |
| 18730D3-6 | 2.03         | 0.764 | 9.55                           | 9.4    | 8.93   | 27.9  | 13.80          |
| 18730D3-4 | 1.97         | 0.764 | 9.49                           | 9.73   | 9.25   | 28.5  | 13.90          |
| 18708B2-2 | 2.01         | 0.763 | 9.54                           | 9.16   | 9.11   | 27.8  | 13.97          |
| 18708B3-4 | 2.01         | 0.760 | 9.53                           | 9.14   | 9.03   | 27.7  | 13.80          |
| 18708B3-5 | 2.02         | 0.766 | 9.79                           | 8.98   | 8.83   | 27.6  | 13.67          |

### **Stability studies**

The a-Si:H/nc-Si:H/nc-Si:H triple-junction modules ( $400 \text{ cm}^2$ ) for the low-rate case (Table II) and triple-junction unencapsulated cells ( $1.1 \text{ cm}^2$ ) high-rate case (Table III) have been light soaked to attain stable values. The stable efficiency of the low-rate modules in Table II is in the range of 10.8-11.3%. The best cell, as measured at USO, showed stable characteristics of  $V_{oc} = 1.90 \text{ V}$ ,  $J_{sc} = 8.52 \text{ mA}/\text{cm}^2$ , FF = 0.699, and efficiency = 11.35%.

The stable active-area efficiency of the high-rate cells in Table III is in the range of 12.4-12.9%. The best cell, as measured at USO, showed stable characteristics of  $V_{oc} = 1.980 \text{ V}$ ,  $J_{sc} = 9.04 \text{ mA}/\text{cm}^2$ , FF = 0.719, and efficiency = 12.86%. Both types of modules/cells have been sent to NREL for confirmation of efficiency, and will be reported when available.

### **CONCLUSIONS**

We have fabricated a-Si:H/nc-Si:H/nc-Si:H triple junction solar cells and modules at low rate ( $<1 \text{ nm/s}$ ) and high rate ( $>1 \text{ nm/s}$ ) using our HF process. The highest initial, aperture-area efficiency attained for  $400 \text{ cm}^2$  encapsulated modules is 12.0%, as confirmed by NREL. The corresponding stable efficiency, as measured at USO, is  $\sim 11.3\%$ . For high rate, small-area ( $1.1 \text{ cm}^2$ ) unencapsulated cells, we have attained initial active-area efficiency of 13.97% and stable efficiency of 12.86%.

### **ACKNOWLEDGMENTS**

The authors thank X. Xu and J. Zhang for important contributions. The authors also thank G. DeMaggio for useful discussions and data analysis, D. Wolf, N. Jackett, L. Sivec, C. Worrel, J. Piner, Y. Zhou, T. Palmer, J. Owens, R. Caraway, and B. Hartman for sample preparation and measurements. The work was supported by US DOE under the Solar America Initiative Program Contract No. DE-FC36-07GO17053.

**REFERENCES**

1. J. Meier, R. Flückiger, H. Keppner, and A. Shah, *Appl. Phys. Lett.* **65**, 860 (1994).
2. B. Yan, G. Yue, and S. Guha, *Mat. Res. Soc. Symp. Proc. Vol.* **989**, 335 (2007).
3. O. Vetterl, F. Finger, R. Carius, P. Hapke, L. Houben, O. Kluth, A. Lambertz, A. Mück, B. Rech and H. Wagner, *Sol. Ener Mater and Sol Cells*, **62**, 97 (2000).
4. X. Xu, Y. Li, S. Ehlert, T. Su, D. Beglau, D. Bobela, G. Yue, B. Yan, J. Zhang, A. Banerjee, J. Yang, and S. Guha, *Mat. Res. Soc. Symp. Proc. Vol.* **1153** (2009).
5. M. Kondo, T. Matsui, Y. Nasuno, C. Niikura, T. Fujibayashi, A. Sato, A. Matsuda, and H. Fujiwara, *Proc. 31<sup>st</sup> IEEE PVSC (IEEE, New York, 2005)*, p. 1377 (and references therein).
6. P. Torres, J. Meier, R. Fluckiger, U. Kroll, J. A. A. Selvan, H. Keppner, A. Shah, S. D. Littlewood, I. E. Kelly, and P. Giannoules, *Appl. Phys. Lett.* **69**, 1373 (1996).

Mater. Res. Soc. Symp. Proc. Vol. 1321 © 2011 Materials Research Society

DOI: 10.1557/opl.2011.803

## THIN FILM SILICON SOLAR CELLS UNDER MODERATE CONCENTRATION

L.M. van Dam, W.G.J.H.M. van Sark, R.E.I. Schropp  
Utrecht University, Faculty of Science, Debye Institute for Nanomaterials Science,  
Nanophotonics - Physics of Devices, P.O. Box 80.000, 3508 TA Utrecht, The Netherlands,  
Tel: 030 253 3170, e-mail: r.e.i.schropp@uu.nl

### ABSTRACT

There are only very few reports on the effects of concentration in thin film silicon-based solar cells. Due to the presence of midgap states, a fast decline in fill factor was observed in earlier work. However, with the advent of more stable and lower defect density polycrystalline silicon materials as well as high quality micro-/nanocrystalline silicon materials, it is worth revisiting the performance of cells with these absorber layers under moderately concentrated sunlight. We determined the behavior of the external  $J$ - $V$  parameters of pre-stabilized substrate-type (n-i-p) amorphous and microcrystalline solar cells under moderate concentrations, between 1 sun and 21 suns, while maintaining the cell temperature at 25°C. It was found that the cell efficiency of both the amorphous and the microcrystalline cells increased with moderate concentration, showing an optimum at approximately 2 suns. Furthermore, the enhancement in efficiency for the microcrystalline cells was larger than for the amorphous cells. We show that the  $V_{oc}$ 's up to 0.63 V can be reached in microcrystalline cells while  $FF$ 's only decrease by 9%. The effects have also been computed using the device simulator ASA, showing qualitative agreement.

### INTRODUCTION

Recently, in the quest for higher efficiencies for thin film solar cells, much emphasis is placed on light trapping or absorption enhancement techniques, such as the use of plasmonic or diffractive back contacts [1] and luminescent concentrators [2], to concentrate the incident light in cells with a thinner absorber layer or with a smaller area. Even in less advanced schemes, merely optical concentration of light can yield higher efficiencies. There are only very few reports on the effects of concentration in thin film silicon-based solar cells [3]. Due to the presence of midgap states, a fast decline in fill factor was observed in earlier work. However, with the advent of more stable and lower defect density polycrystalline silicon materials as well as high quality micro-/nanocrystalline silicon materials, as well as the increasing concentration ratios obtained by novel light management techniques, it is worth revisiting the performance of cells with these absorber layers under moderately concentrated sunlight. Furthermore, local generation rates in thin film silicon solar cells with a plasmonic back reflector are much enhanced and the study of the effect of external optical concentration can help to optimize their design.

We determined the behavior of the external  $J$ - $V$  parameters of pre-stabilized substrate-type (n-i-p) amorphous and microcrystalline solar cells under moderate concentrations, between 1 sun and 21 suns, while maintaining the cell temperature at 25°C. Maintaining the cell temperature is an important requirement when measuring under concentrated illumination, because rapidly increasing temperatures can influence the  $J$ - $V$  measurement and too high temperatures can damage the cell [4]. We apply extensive active cooling by means of Peltier devices and selected solar cells deposited in the substrate (n-i-p) configuration on stainless steel, because they can be cooled very accurately at the rear side of the substrate, while maintaining easy access to the electrical contacts. It should be noted that these cells already comprise some sort of local light concentration due to the use of textured surfaces.

In addition, we computed  $J$ - $V$  characteristics using the one-dimensional model for semiconductor device simulation ASA, which is a product of the Delft University of Technology [5]. Simulations were performed with cell parameters approximating the measured cells and illuminations between 1 sun and 21 suns.

## METHODS AND MATERIALS

Two types of thin-film photovoltaic cells were investigated: a single junction hydrogenated amorphous silicon cell (a-Si:H) and a single junction hydrogenated microcrystalline silicon cell ( $\mu$ c-Si:H), both in substrate (n-i-p) configuration. The intrinsic layer in the a-Si:H cell had protocrystalline nature. The estimated thicknesses of the n, i and p layer of the amorphous silicon cells were 80 nm, 500 nm, and 20 nm, respectively, and were deposited at 195°C, 250°C, and 160°C, respectively. The intrinsic layer was deposited by Hot-Wire Chemical Vapor Deposition. The estimated thicknesses of the n, i and p layer of the microcrystalline silicon cells were 27 nm, 2000 nm and 20 nm, respectively. The i-layer was deposited by Hot-Wire Chemical Vapor Deposition at a temperature of 250°C, the other layers at 195°C. The microcrystalline cells were applied on a stainless steel substrate and have an Ag and ZnO back reflecting contact. The square cells have either a V-shaped top contact or a grid-type contact. In both cases, the total area is 16 mm<sup>2</sup> and the active area is 13 mm<sup>2</sup>.

AM1.5 light was produced by a WACOM dual source solar simulator, which has a uniformity of the irradiated area within  $\pm 3\%$ , an illumination stability of  $< 1\%$  reproducibility and a spectral match of  $\pm 3.0\%$  for 350-500 nm,  $\pm 2.0\%$  for 500 – 800 nm and 4.5% for 800 – 1100 nm [6]. Increasing the light intensity was done by means of a polymer hybrid Fresnel-prismatic lens, a lens with a surface that partly consists of square planes and partly of curved planes to refract the light. The dimensions of the lens are 160 mm by 160 mm. This lens (initially developed for use in a concentrating photovoltaic module [7]) was kindly supplied by the Italian National Agency for New Technologies, Energy and sustainable economic development (ENEA) and has a transparency of 82-83% according to their specifications [8]. This lens was mounted on a labjack between the solar simulator and the solar cells. The illumination intensity (concentration ratio) of the incident light on the cell was varied by varying the distance ( $x$ ) between the lens and the solar cell, where  $x <$  the focal distance of the lens ( $f$ ) (Figure 1).

Calibration of the light intensity was done with the use of a Coherent Inc. LaserCheck, a hand-held laser power density meter. This device was placed at the location of the solar cells and the light intensity was measured with the lens at a range of distances. Comparing the measured light intensities with the measured light intensity at 1 sun provided the intensity in relation to the distance to the lens. To protect the power density meter, a neutral density filter of 10% transparency was used. The results were fitted to a simple power function with an  $R^2$  of 0.9997 to provide continuous data.

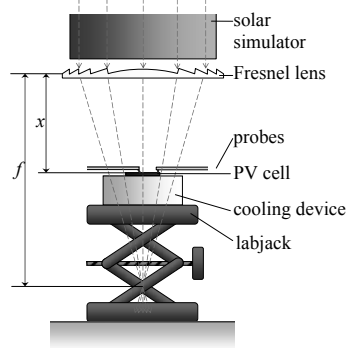


**Figure 1.** Schematic drawing of the measurement setup, showing the light path from the solar simulator, passing through the Fresnel lens where it is converged and reaches the PV cell. The labjack is used to modify the distance from the lens to the cell ( $x$ ). Distance  $f$  is the focal distance of the lens.



Cooling of the solar cells by merely forcing a stream of ambient air of approximately 17°C along the solar cell proved to be insufficient. The substrate configuration of the solar cells provided the possibility to actively cool the cells at the stainless steel back side. In addition, the stainless steel substrate of the cells helps to disperse the heat and to stabilize the temperature of the cell. The cells were attached to an aluminum slab with the use of a heat sink compound to ease the transfer of heat from the stainless steel substrate to the aluminum slab. On the other side of the slab, two PolarTEC Peltier devices were attached to actively extract a maximum of 83.4 W of heat each from the block. Two CoolerMaster Hyper 101 convector cooling units, each capable of removing a maximum of 100 W heat, disposed of the heat from the Peltier devices. A Newport Electronics thermal control unit measured the cell temperature by means of a thermocouple wire on the stainless steel substrate and activated the Peltier devices. This way, the temperature could be kept within the range of 24.5 – 25.0°C at all times. Illuminated  $J$ - $V$  characteristics were measured by a Keithley 238 source-measure unit using a four point probe configuration at a voltage between -0.3 V and 1.0 V in steps of 100 mV.

The input parameters for the simulations were defined by a standardized amorphous photovoltaic cell in a superstrate configuration from Delft University of Technology, which were adapted to have an approximate match to the specific amorphous solar cell that was used for the measurements. This was done in the settings file by removing the glass and the transparent conductive oxide (TCO) layer (because we were using substrate type cells) and adjusting the thickness of the p, i and n layers. The light intensity was varied by multiplying the input spectrum, AM1.5, 100 mW/cm<sup>2</sup>, by 1 to 21.

## RESULTS AND DISCUSSION

### Measurements

The measured illuminated  $J$ - $V$  characteristics of both the amorphous and the microcrystalline silicon cells are shown in figures 2a and 2b, respectively, both normalized to the  $J_{sc}$  of their individual reference measurement under standard AM1.5, 100 mW/cm<sup>2</sup> conditions. The arrows in the graphs indicate the trends when increasing the illumination intensity. Both the amorphous and the microcrystalline silicon cells show an increase in  $V_{oc}$ , but the amorphous silicon cell shows in addition a strong change in the curvature, affecting the fill factor. The decrease in fill factor for the microcrystalline silicon cells is

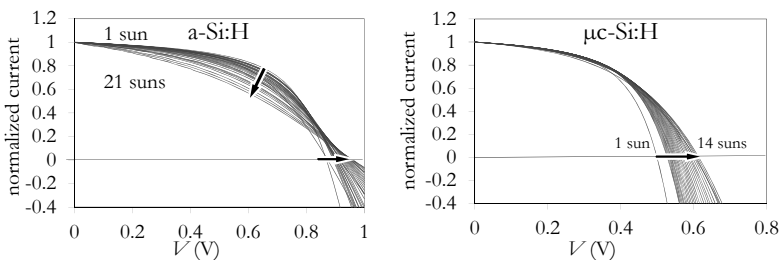


**Figure 2.** Measured  $J$ - $V$  curves of the a-Si:H cell G6 (a) and the  $\mu$ c-Si:H cell I6 (b) at light intensities ranging from, respectively, 1 to 21 suns and 1 to 14 suns. The measured current densities are normalized to the  $J_{sc}$  of their respective reference measurement under standard AM1.5, 100 mW/cm<sup>2</sup> conditions.

significantly smaller than that for the amorphous silicon cells. The fill factor of the amorphous silicon cell drops from 0.56 (at 1 sun) to 0.41 (at 14 suns), a drop of 27%, whereas the fill factor of the microcrystalline cell only drops from 0.55 (at 1 sun) to 0.46 (at 14 suns), a drop of only 16%. The relative gain in  $V_{oc}$  for the  $\mu\text{-Si:H}$  solar cell is considerably higher than that for the a-Si:H cell. Studied over the intensity range of 1 to 14 suns, the gain is 21%, while that for a-Si:H cells is only 9.0%. This is also depicted in figures 3a and 3b, where both the  $V_{oc}$  and the fill factor are plotted versus the light intensity.

The measurements show that the  $V_{oc}$  of the a-Si:H cells increases logarithmically from 0.87 V at 1 sun to a maximum close to 1.0 V at the highest intensity studied. The  $\mu\text{-Si:H}$  cells show a similar behavior, only the increase in  $V_{oc}$  is more remarkable, i.e., 22% from 0.50 V at 1 sun to 0.61 V at 12 suns. When the AM1.5 efficiencies, calculated from the  $J-V$  characteristics and the calibrations, are plotted, both the amorphous and the microcrystalline silicon cells show an increase in efficiency, which is optimal at a light intensity of around 2 suns (Figure 4). The efficiency of the a-Si:H cells appears to have an optimum at a relative illumination of 1.9 times AM1.5, peaking at 7.3%, where the standard one sun efficiency is measured at 5.5%. At higher light intensities, the efficiency decreases.

For the  $\mu\text{-Si:H}$  cells, the peak efficiency is measured at 9.4% at a relative illumination of 2.1 times AM1.5, where the standard one sun efficiency is measured to be 7.1%.

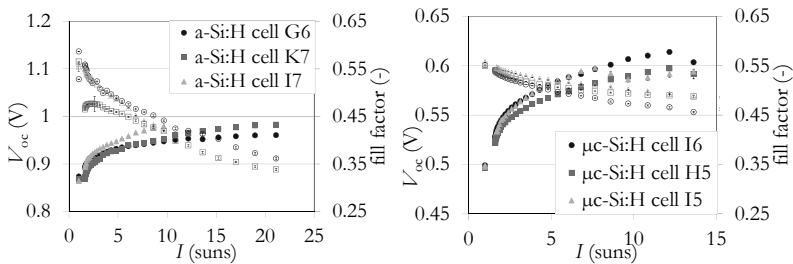


**Figure 3.**  $V_{oc}$  and fill factor plotted versus the light intensity for the measured a-Si:H cells (a) and  $\mu\text{-Si:H}$  cells (b). Filled markers show the  $V_{oc}$ , open markers show the fill factor.

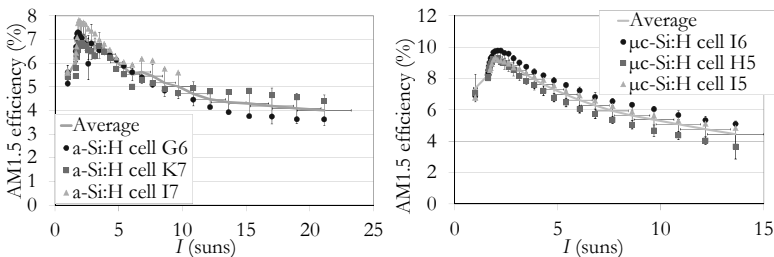


**Figure 4.** AM1.5 efficiencies plotted versus the light intensity (a) for the measured a-Si:H cells (b) and  $\mu\text{-Si:H}$  cells.